

Steady state pressure driven fluid flow in a cylindrical tube filled with bidisperse porous medium

Basant K. Jha, Muhammad K. Musa*

Department of Mathematics, Ahmadu Bello University, Zaria 810001, Nigeria

Corresponding Author Email: mmkabirxy@yahoo.com

<https://doi.org/10.18280/ijht.360434>

ABSTRACT

Received: 20 January 2018

Accepted: 17 October 2018

Keywords:

applied constant pressure gradient, Bidisperse porous medium, coefficient of momentum transfer, D'Alembert method, Horizontal tube

This article presents a model for fluid flow in a cylindrical tube filled with a Bi-disperse Porous Medium (BDPM). The model is a modified Brinkman model where the conventional single solid porous structure is replaced with a porous matrix having a dual porous phases (the fracture and porous phases). The fluid velocities U_f and U_p in the fracture and porous phases respectively of the BDPM are coupled together by the coefficient of momentum transfer (η). Exact solutions in terms of modified Bessel functions for the velocity fields in the fracture and porous phases for any arbitrary value of η using D'Alembert method as well as for the limiting cases $\eta = 0$ and $\eta \rightarrow \infty$ have been obtained. The study establishes that increasing the momentum transfer coefficient suppresses (enhances) the fluid velocity in the fracture (porous) phases of the BDPM.

1. INTRODUCTION

A porous material is described as material that is made up of a solid matrix with an interconnected pores. The interconnectedness of the pores allow the flow of one or more fluids through the material. The role plays by porous media in any transport problem bore out of its two important properties: measure of permeability and the ratio of all the pores to the total volume of the medium (porosity). Jha and Musa [1-2] noted that if the permeability of the porous medium is increased, the fluid experiences less resistance to motion and consequently, increase in the fluid momentum is observed. By taking the effect of porosity into account, Vortmeyer and Schuster [3] observe that the flow channeling will naturally occur adjacent to the surface of the transport medium. In addition, the effect of variable porosity on fluid flow in a vertical channel filled with porous material was also investigated by Paul et al. [4]. Several researchers such as Vafai and Tien [5] and Vafai [6] have documented the influence of porous media on fluid flow. Additionally, Butler et al. [7] studied the interstitial fluid flow in biological tissues such as the fibrous tissues connecting bones and cartilages when subjected to tension.

Diverse applications of porous media have been recorded and each application may necessitate the use of a different form of porous structure. For instance, Warren and Root [8] examined the problems related to fractured porous medium where the porous structure consist of two superimposed continuum fracture system (Double porosity medium or DPM). The understanding of the roles play by the fracture properties in this type of porous structure are of great scientific interest, especially as they strongly influence fluid flow such as underground fluid flow or contaminants. More so, the abundance of fracture material increases the area of application from the initially industrial application to wider areas such as the petroleum, geothermal and water supply reservoirs. Thus, in the determination of the up-scaled inter-block transmissibility in DPM, Arbogast et al [9] derived the

mathematical model for Double Porosity Model of single phase flow. Results on DPM and general porous media can also be found in Avraam and Payatakes [10], Dietrich et al [11], Hassanizadeh and Gray [12], the excellent work of Bourgeat [13] et al. on the double porosity model for immiscible incompressible two-phase flow in a reduced pressure formulation. Other investigations include the texts of Kaviany [14] and Nield and Bejan [15] where the problems of fluid flow in the presence of porous medium are extensively discussed.

In industrial applications where large area for liquid firm evaporation, such as in the evaporators of heat pipes are required, the use of a Bi-Disperse Porous Media (BDPM) has been proposed [16]. In a theoretical and experimental study on stagnant thermal conductivity of Bi-disperse porous media, Chen et al. [17] stated that a BDPM can be viewed as a case where the traditional classical porous medium is replaced with another form of porous structure consisting of two phases: the macro-void (fracture or f-phase) and a micro-pore (porous or p-phase). Modifying the Brinkman model, Nield and Kuznetsov [18] proposed a model for the steady-state momentum transfer in a BDPM. The model consists of a pair of second order differential equation in which the velocities profiles (for the fracture and porous phases) are coupled together by a parameter; the coefficient of momentum transfer. Nield and Kuznetsov [19] observe that the inclusion of the coefficient of momentum transfer in the model is simply to modify the permeabilities of the two phases of the BDPM via the parameter $\left(\frac{\zeta}{\mu}\right)$; where ζ is the dimensional velocity transfer coefficient and μ represents the fluid viscosity.

In this article, a mathematical model is presented for the fluid flow resulting from the application of a constant negative pressure gradient in the z-direction (Fig. 1.0) on a viscous, incompressible fluid in a horizontal cylindrical tube filled with Bidisperse porous medium. The exact solutions in terms of modified Bessel functions for the velocity profiles in

both the fracture and porous phases have been obtained while taking into account the role of the parameter that couple the two velocity profiles together. Accordingly, three cases are considered: (i) the general fluid flow for any arbitrary value of the momentum transfer coefficient. In this case, the second order governing differential equations are systematically decoupled without altering the initial order of the equation. (ii) the weak coupling: when the coefficient of momentum transfer is neglected and (iii) the strong coupling; when the momentum transfer coefficient approaches infinity.

2. MATHEMATICAL ANALYSIS

Consider a steady state fluid flow formation emanating from the applied constant pressure gradient on fluid of constant density (ρ) and viscosity (μ) in a horizontal pipe filled with Bidisperse Porous Material as displayed in figure 1.0 below.

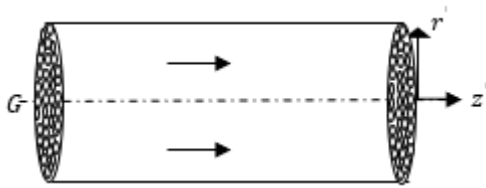


Figure 1. Schematic diagram of the problem

Assume that the pipe is open on both ends, the fluid flows along the direction of z -axis and also the radius of the cylinder is finite when $r = a$. Following Niell and Kuznetsov [18] and Magyari [20], the mathematical model that describes the physical situation of the fully developed stable fluid flow formation through a horizontal tube in dimensional forms are given by:

$$G = \frac{\mu}{k_f} U_f' + \zeta(U_f' - U_p') - \bar{\mu}_f \frac{1}{r'} \frac{d}{dr'} \left(r' \frac{dU_f'}{dr'} \right) \quad (1)$$

$$G = \frac{\mu}{k_p} U_p' + \zeta(U_p' - U_f') - \bar{\mu}_p \frac{1}{r'} \frac{d}{dr'} \left(r' \frac{dU_p'}{dr'} \right) \quad (2)$$

where U_f' and U_p' represent the fluid velocity in the fracture and porous phases respectively along the z -axis. Here, $G = \frac{dp}{dz}$ is the negative applied constant pressure gradient which induces the fluid flow formation. Thus, in this set up, the boundary conditions consistent with this work are taken to be:

$$\left. \begin{aligned} \frac{dU_f'}{dr'} = \frac{dU_p'}{dr'} = 0 & \quad \text{at } r' = 0 \\ U_f' = U_p' = 0 & \quad \text{at } r' = a \end{aligned} \right\} \quad (3)$$

Using the non-dimensional quantities defined below in Eqs(1)-(3):

$$R = \frac{r'}{a}, Da_f = \frac{k_f}{a^2}, Da_p = \frac{k_p}{a^2}, \eta = \zeta \frac{a^2}{\mu}, \gamma_f = \frac{\bar{\mu}_f}{\mu}, \gamma_p = \frac{\bar{\mu}_p}{\mu}, U_f = \frac{\mu U_f'}{a^2 G}, \text{ and } U_p = \frac{\mu U_p'}{a^2 G}$$

The mathematical model will now reduced to:

$$\frac{\gamma_f}{R} \frac{d}{dR} \left(R \frac{dU_f}{dR} \right) - \eta(U_f - U_p) - \frac{U_f}{Da_f} = -1 \quad (4)$$

$$\frac{\gamma_p}{R} \frac{d}{dR} \left(R \frac{dU_p}{dR} \right) - \eta(U_p - U_f) - \frac{U_p}{Da_p} = -1 \quad (5)$$

The corresponding boundary conditions are:

$$\left. \begin{aligned} \frac{dU_f}{dR} = \frac{dU_p}{dR} = 0 & \quad \text{at } R = 0 \\ U_f = U_p = 0 & \quad \text{at } R = 1 \end{aligned} \right\} \quad (6)$$

Clearly, the complexity in obtaining the exact solutions for Eqs (4) and (5) will naturally originate from the coefficient of momentum transfer (η). Niell and Kuznetsov [19] obtained an exact solution by directly eliminating one of the velocities. This approach results into rising the power of the governing equations to a fourth order differential equation. Attempting to avoid this complication, Cheng [21] adopted the cubic spline collocation method. Magyari [20], while investigating the high speed channel flow in a Bidisperse porous medium employed the reduction to normal mode method. In this classical mechanics approach, the simplified governing equations are transformed into matrix form, then followed by matrix-similarity transformation. In this present work, the exact solutions of the coupled governing equations are obtained for any arbitrary value (general case) of the coupling parameter (η) using the D'Alembert method (Ziyaddin and Huseyin [22]). The choice of this method is to allow for the systematic decoupling of the governing equations while still retaining their initial orders.

2.1 General case

Multiplying Eq(4) by A , adding the resulting equation to Eq(5) and simplifying the final equation yields

$$\frac{1}{R} \frac{d}{dR} \left(R \frac{d}{dR} (AU_f + U_p) \right) - \delta^2 (AU_f + U_p) = - \left(\frac{A\gamma_p + \gamma_f}{\gamma_f \gamma_p} \right) \quad (7)$$

where

$$A = \frac{Da_p(A\gamma_p + A\eta\gamma_p Da_f - \eta\gamma_f Da_f)}{Da_f(\gamma_f + \eta\gamma_f Da_p - \eta A\gamma_p Da_p)} \quad (8)$$

$$\delta^2 = \frac{\eta}{\gamma_p} - \frac{\eta A}{\gamma_f} + \frac{1}{\gamma_p Da_p} \quad (9)$$

The particular solution of Eq(7) subject to the boundary conditions (Eq(6)) in terms of modified Bessel function of the first kind assumes the following form:

$$AU_f + U_p = \frac{\gamma_f + A\gamma_p}{\delta^2 \gamma_f \gamma_p} \left(1 - \frac{I_0(R\delta)}{I_0(\delta)} \right) \quad (10)$$

Replacing A and δ in Eq(10) with their respective roots:

$$A_1 = \frac{1}{2}(d_1 + d_2) \quad (11a)$$

$$A_2 = \frac{1}{2}(d_1 - d_2) \quad (11b)$$

$$\delta_1 = \sqrt{\frac{1}{Da_p \gamma_p} + \frac{\eta}{\gamma_p} - \frac{\eta A_1}{\gamma_f}} \quad (12a)$$

$$\delta_2 = -\sqrt{\frac{1}{Da_p \gamma_p} + \frac{\eta}{\gamma_p} - \frac{\eta A_2}{\gamma_f}} \quad (12b)$$

obtained from Eqs (8) and (9), the expressions for the velocity profiles in the fracture and porous phases are separately obtained as follows:

$$U_f = \frac{1}{A_1 - A_2} \left[d_3 \left(1 - \frac{I_0(R\delta_1)}{I_0(\delta_1)} \right) - d_4 \left(1 - \frac{I_0(R\delta_2)}{I_0(\delta_2)} \right) \right] \quad (13)$$

$$U_p = \frac{1}{A_1 - A_2} \left[A_1 d_4 \left(1 - \frac{I_0(R\delta_2)}{I_0(\delta_2)} \right) - A_2 d_3 \left(1 - \frac{I_0(R\delta_1)}{I_0(\delta_1)} \right) \right] \quad (14)$$

2.2 Weak coupling

If the coefficient of momentum transfer is neglected ($\eta = 0$), Eqs (4) and (5) reduced to two similar equations:

$$\frac{1}{R} \frac{d}{dR} \left(R \frac{dU_f}{dR} \right) - \frac{U_f}{\gamma_f Da_f} = -\frac{1}{\gamma_f} \quad (15)$$

$$\frac{1}{R} \frac{d}{dR} \left(R \frac{dU_p}{dR} \right) - \frac{U_p}{\gamma_p Da_p} = -\frac{1}{\gamma_p} \quad (16)$$

The exact solutions for the velocities profiles of the fracture and porous phases in modified Bessel function obtained by solving Eqs (15) and (16) for $\eta = 0$ subject to the boundary constraints (Eq(6)) are respectively given as:

$$U_f = Da_f \left(1 - \frac{I_0(Rd_5)}{I_0(d_5)} \right) \quad (17)$$

$$U_p = Da_p \left(1 - \frac{I_0(Rd_6)}{I_0(d_6)} \right) \quad (18)$$

2.3 Strong coupling

Also, if the momentum transfer term is large enough, ($\eta \rightarrow \infty$) and by taking η to the order η^{-1} , the velocity fields for both the fractured and the porous phases coincide so that $U_f(Z) = U_p(Z) = U(Z)$. Thus Eqs (4) and (5) respectively are reduced to:

$$\frac{1}{\eta} \frac{1}{R} \frac{d}{dR} \left(R \frac{dU}{dR} \right) - \frac{U}{\gamma_f \eta Da_f} = -\frac{1}{\gamma_f \eta} \quad (19)$$

$$\frac{1}{\eta} \frac{1}{R} \frac{d}{dR} \left(R \frac{dU}{dR} \right) - \frac{U}{\gamma_p \eta Da_p} = -\frac{1}{\gamma_p \eta} \quad (20)$$

Adding and simplifying these equations give:

$$\frac{1}{\eta} \frac{1}{R} \frac{d}{dR} \left(R \frac{dU}{dR} \right) - \frac{U}{2\eta} [d_7] = -\frac{1}{2\eta} \left[\frac{\gamma_f + \gamma_p}{\gamma_f \gamma_p} \right] \quad (21)$$

Solving Eq(21) subject to Eq(6) yields the expression for the fluid momentum when $\eta \rightarrow \infty$ as:

$$U = \frac{Da_f Da_p (\gamma_f + \gamma_p)}{Da_f \gamma_f + Da_p \gamma_p} \left(1 - \frac{I_0(R\sqrt{d_7})}{I_0(\sqrt{d_7})} \right) \quad (22)$$

3. SKIN FRICTION

By differentiating Eqs (14) and (15) and substituting $R = 1$, the expressions for the skin frictions ($\tau_1 = \frac{dU_f}{dR} \Big|_{R=1}$ and $\tau_1 = \frac{dU_f}{dR} \Big|_{R=1}$) for the two phases are:

$$\tau_1 = \frac{1}{(A_1 - A_2)} \left[\frac{\gamma_f + A_1 \gamma_p}{\delta_2 \gamma_f \gamma_p} \left(\frac{I_1(\delta_2)}{I_0(\delta_2)} \right) - \frac{\gamma_f + A_1 \gamma_p}{\delta_1 \gamma_f \gamma_p} \left(\frac{I_1(\delta_1)}{I_0(\delta_1)} \right) \right] \quad (27)$$

$$\tau_1 = \frac{1}{(A_1 - A_2)} \left[\frac{A_2 (\gamma_f + A_1 \gamma_p)}{\delta_1 \gamma_f \gamma_p} \left(\frac{I_1(\delta_1)}{I_0(\delta_1)} \right) - \frac{A_1 (\gamma_f + A_1 \gamma_p)}{\delta_2 \gamma_f \gamma_p} \left(\frac{I_1(\delta_2)}{I_0(\delta_2)} \right) \right] \quad (28)$$

4. RESULTS AND DISCUSSION

In this work, the effects of the Darcy numbers (Da_f and Da_p), ratio of viscosities (γ_f and γ_p) and coefficient of momentum transfer (η) on the fluid momentum and the skin friction at the fluid-surface region are investigated. Accordingly, in order to effectively discuss the effects of these controlling parameters on the velocities as well as on the resulting skin frictions in both the fracture and porous phases, numerical simulation over a reasonable range of values of these parameters have been conducted. Furthermore, for the purpose of comparison, the range of values considered are carefully selected so as to include the values Nield and Kuznetsov [16] refers to as “representative values”.

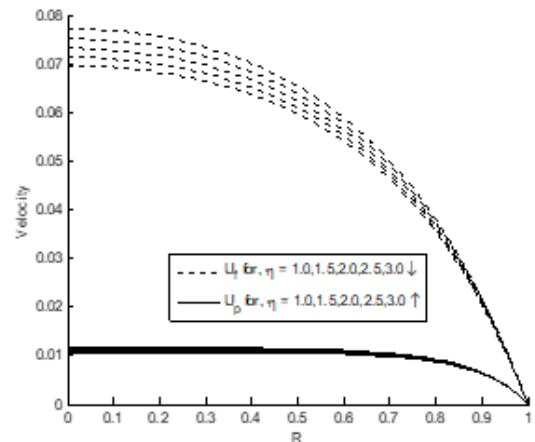


Figure 2. Velocity profile for different values of η and $Da_f=0.1$, $Da_p=0.01$ & $\gamma_f=\gamma_p=1.0$

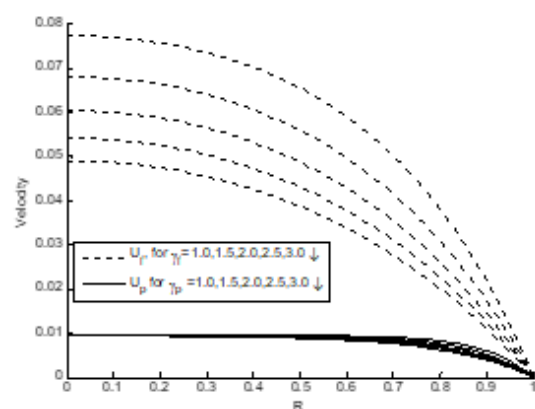


Figure 3. Velocity profile for different values of γ_f and γ_p and $Da_f=0.1$, $Da_p=0.01$ & $\eta=1.0$

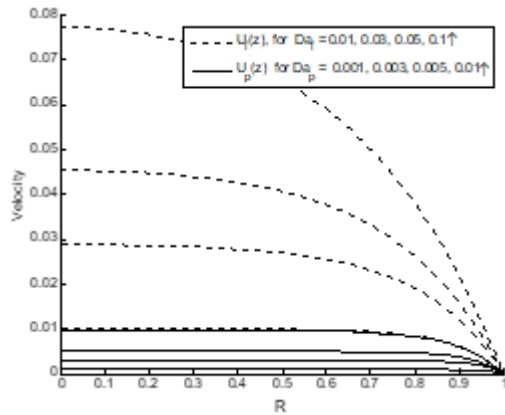


Figure 4. Velocity profile for different values of Da_f and Da_p and $\gamma_f = \gamma_p = 1.0$, & $\eta = 1.0$

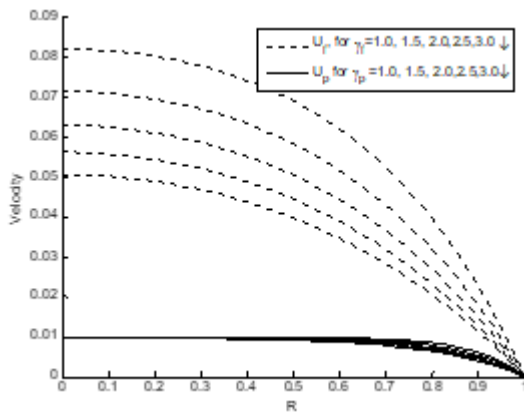


Figure 5. Velocity for different values of γ_f and γ_p with $Da_f = 0.1$, $Da_p = 0.01$

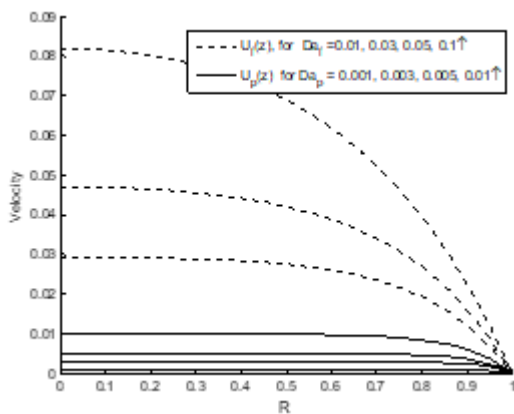


Figure 6. Velocity for different values of Da_f and Da_p with $\gamma_f = \gamma_p = 1.0$

Figure 2.0 shows the velocity distribution for different values of coefficient of momentum transfer (η) with Nield and Kuznetsov's [16] representative values: $Da_f = 0.1$, $Da_p = 0.01$, $\gamma_f = 1.0$ and $\gamma_p = 1.0$. It is found that the fluid momentum is higher in the fracture phase as expected. Furthermore, there is a decrease in the fluid velocity in the fracture phase of the BDPM as the momentum transfer coefficient (η) is increased while a converse trend is observed in the porous phase of the BDPM with respect to the increase in η . The reasons for this opposing flow patterns in the two phases can be clearly seen from Eqs (4 and 5). The

measure of permeability in the fracture phase is higher than that in the porous phase ($Da_f > Da_p$) as a result, the velocity distributions; $U_f > U_p$. From Eq(4), it is clear that $(U_f - U_p) > 0$ so that increasing the momentum transfer coefficient ($\eta > 0$) on the fluid momentum will naturally attenuate the velocity strength of the fluid in the fracture phase. On the other hand, from Eq(5), it is observed that the quantity $(U_p - U_f) < 0$ so that the overall effect resulting from the increase in η enhances the fluid velocity in the porous phase of the BDPM. To further validate these flow patterns, the numerical values generated from the work on normal mode analysis of high speed channel flow in a BDPM (Magyari [20]) are compared with those in this present research (table 1.0) using $Da_f = 0.1$, $Da_p = 0.01$ and $\gamma_f = \gamma_p = 1.0$. From the table, it is observed that the flow patterns in the fracture and porous phases in Magyari [20] favourably agree with the flow patterns in the present work.

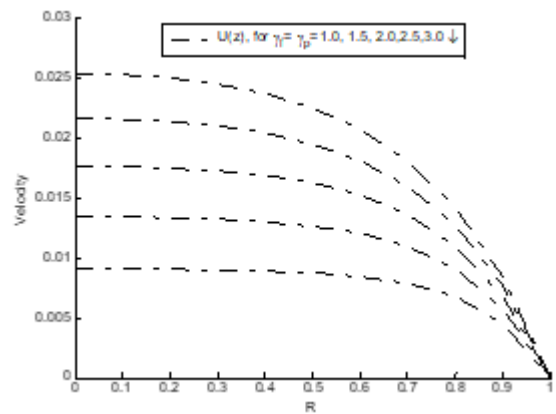


Figure 7. Velocity profile for different values of γ_f and γ_p and $Da_f = 0.1$, $Da_p = 0.01$

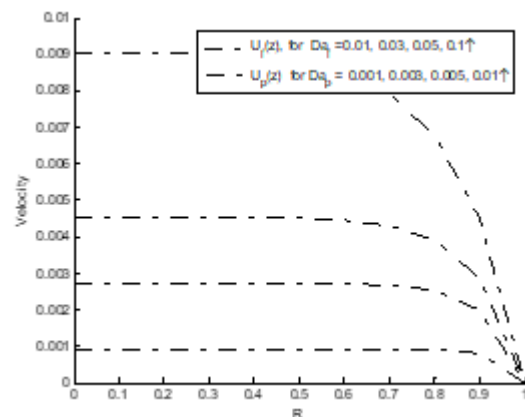


Figure 8. Velocity profile for different values of Da_f and Da_p and $\gamma_f = \gamma_p = 1.0$

The velocity distribution with respect of the ratio of viscosity of the fluid is displayed in figures 3.0 (general case), 5.0 (weak coupling) and 7.0 (strong coupling). If the ratio of the viscosity of the fluid is high, the fluid becomes thicker. Hence, the resistance of the fluid to motion resulting from the applied constant pressure gradient is increased. Therefore, a decrease in the fluid velocity is observed in all the three figures. Also, the effect of the variations of γ_f and γ_p in the porous phase (figures 3.0 and 5.0) from the centerline of the tube ($R = 0$) up to near $R = 0.4$ is seen to be insignificant as evidently seen from the strength lines in the graphs. Close to

the curved surface of the cylinder (after $R = 0.6$), the effects of the variation of the fluid's ratio of viscosities become visibly noticed. The velocity distribution for different values of Darcy numbers with fix values of $\gamma_f = \gamma_p = 1.0$ are depicted in figure 4.0 when $\eta = 1.0$, figure 6.0 when $\eta = 0$ and figure 8.0 when $\eta \rightarrow \infty$. From these figures, it is observed that the velocity distribution in the fracture and porous phases of the BDPM increases with increase in Darcy numbers. This is expected because increasing the measure of permeability (Da) of the BDPM lead to increasing the pores of the porous passages. This result to the decrease in the frictional force between the porous matrix and the flowing fluid hence the increase in velocity strength of the fluid.

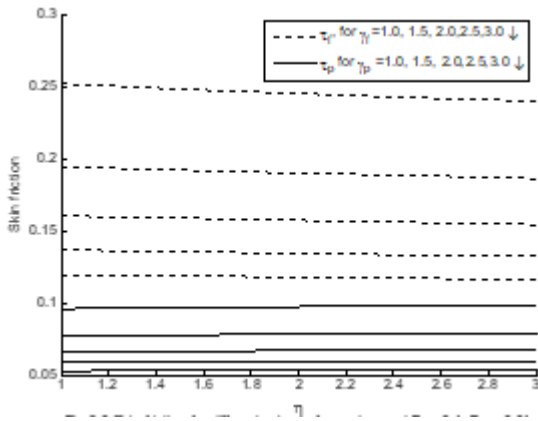


Figure 9. Skin friction for different values of γ_f and γ_p and $Da_f=0.1, Da_p=0.01$

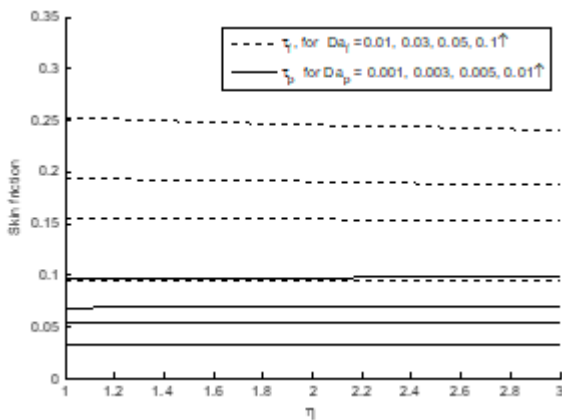


Figure 10. Skin friction for different values of Da_f and Da_p & $\gamma_f=\gamma_p=1.0$

Eqs (27) and (28) express the skin friction at the fluid-wall region for any arbitrary value of the coefficient of velocity transfer (η). The effects of the controlling parameters on the skin friction in the two phases of the BDPM are depicted in figures 9.0 and 10.0. For $Da_f = 0.1$ and $Da_p = 0.01$, the skin friction is noticed to decrease with increase in γ_f and γ_p in both phases. In addition, the skin friction is also observed to be decreasing steeply in the fracture phase as the coefficient of momentum transfer (η) is increased. In figure 10.0, at fix values of $\gamma_f = \gamma_p = 1.0$, the influence of the variation of Darcy numbers on the skin friction in the two phases is displayed. It is observed that the skin friction decreases with η but increases with Da_f and Da_p in the fracture phase of BDPM. In both figures 9.0 and 10.0, the effect of the variation of coefficient of momentum

transfer (η) on the skin friction in the porous phase is negligible as can be notice from the straight line parallel to the η -axis.

4. CONCLUSION

In this paper, the mathematical model for fluid flow inside a cylindrical tube filled with Bidisperse Porous Material has been developed and exact solution obtained in terms of modified Bessel functions. Special interest has been placed on the effect of the parameter that couples the velocities of the fluid in the two phases together. D'Alembert method was used to obtain the expressions for the velocity profiles for any arbitrary value of the momentum transfer coefficient. This investigation establishes that the ratio of viscosities of the fluid γ_f and γ_p generally suppresses the fluid momentum while the coefficient of momentum transfer (η) is found to attenuates the fluid velocity in the fracture phase and aids the velocity distribution in the porous phase of the BDPM. Furthermore, the increase in the measure of permeabilities of the porous medium enhance the fluid momentum. It is further found that skin friction increases with Da_f and Da_p but decreases with increase in γ_f and γ_p and the coefficient of momentum transfer (η).

REFERENCES

- [1] Jha BK, Musa MK. (2011). Time dependent natural convection Couette flow of heat generating/absorbing. Fluid between infinite vertical Parallel plates filled with Porous material. Journal of the Nig. Association of Mathematical Physics 19(2011): 233-248.
- [2] Jha BK, Musa MK. (2012). Unsteady natural convection Couette flow of heat generating/absorbing fluid between infinite vertical Parallel plates filled with porous material. Appl. Math Mech. (English. Ed) 33(3): 303-314. <https://doi.org/10.1007/s10483-012-1551-8>
- [3] Vortmeyer D, Schuster J. (1983): Evaluation of steady flow profile in a rectangular and circular packed beds. Chem. Engng. Sci. 38(1983): 1691-1699. [https://doi.org/10.1016/0009-2509\(83\)85026-X](https://doi.org/10.1016/0009-2509(83)85026-X)
- [4] Paul T, Singh AK, Mishra AK. (2001). Transient natural convection between two vertical walls filled with a porous material having variable porosity. Math, Engng. Ind. 8(3): 177-185.
- [5] Vafai K, Tien CL. (1981). Boundary and inertia effects on flow and heat transfer in porous media. Intl. J. Heat Mass Transfer 24(1981): 195-203. [http://dx.doi.org/10.1016/0017-9310\(81\)90027-2](http://dx.doi.org/10.1016/0017-9310(81)90027-2)
- [6] Vafai K. (1984). Convective flow and heat transfer in variable-porosity media. Journal of Fluid Mech. 147(1984): 233-259. <http://dx.doi.org/10.1017/S002211208400207X>
- [7] Butler SL, Kohles SS, Thielke RJ, Chen C, Vanderby R. (1997). Interstitial fluid flow in tendons or ligaments: A porous medium finite element simulation. Med. Biol, Eng. Comput. 35(1997): 742-746. <http://dx.doi.org/10.1007/BF02510987>
- [8] Warren J, Root P. (1963). The behavior of naturally fractured reservoirs. Soc. Petrol. Eng. J. 3(1963): 245-255. <http://dx.doi.org/10.2118/426-PA>

[9] Arbogast T, Douglas J, Hornung U. (1990). Derivation of the double porosity model of single phase flow via homogenization theory. *SIAM J. Math. Anal.* 21(1990): 823-836. <http://dx.doi.org/10.1137/0521046>

[10] Avraam DG, Payatakes AC. (1995). Generalized relative permeability coefficients during steady state two- phase flow in porous media, correlation with flow mechanisms. *Transport in Porous Media* 20(1): 135-168. <https://doi.org/10.1007/BF00616928>

[11] Dietrich P, Helming R, Sauter M, Hölzl H, Köngeter J, Teutsch G. (2005). *Flow and transport in fractured porous media.* Springer Verlag. <http://dx.doi.org/10.1007/b138453>

[12] Hassanizadeh SM, Gray WG. (1990). Mechanics and thermodynamics of multiphase flow in porous media including interphase boundaries. *Adv. Water Resour* 13(1990): 169-186. [http://dx.doi.org/10.1016/0309-1708\(90\)90040-B](http://dx.doi.org/10.1016/0309-1708(90)90040-B)

[13] Bourgeat A, Luckhaus S, Mikelić A. (1996). Convergence of the homogenization process for a double-porosity model of immiscible two-phase flow. *SIAM J. Math. Anal.* 27(1996): 1520–1543. <http://dx.doi.org/10.1137/S0036141094276457>

[14] Kaviany K. (1991). *Principle of heat transfer in porous media.* Springer-Verlog, New York. <http://dx.doi.org/10.1007/978-1-4684-0412-8>

[15] Nield DA, Bejan A. (1999). *Convection in porous media.* 2nd Ed. Springer-Verlog, New York.

[16] Nield DA, Kuznetsov AV. (2013). A note on modelling high speed flow in a Bidisperse porous medium. *Transport Porous Medium* 96(2013): 495-499. <https://doi.org/10.1007/s11242-012-0102-1>

[17] Chen ZQ, Cheng P, Hsu CT. (2000). A theoretical and experimental study on stagnant thermal conductivity of Bi-disperse porous media. *Int. Commun. Heat Mass Transfer* 27(2000): 601-610. [https://doi.org/10.1016/S0735-1933\(00\)00142-1](https://doi.org/10.1016/S0735-1933(00)00142-1)

[18] Nield DA, Kuznetsov AV. (2005). A two velocity two temperature model for a Bidisperse porous medium: Forced convection in a channel. *Transport Porous Medium* 59(2005): 325-339. <http://dx.doi.org/10.1007/s11242-004-1685-y>

[19] Nield DA, Kuznetsov AV. (2011). Forced convection in a channel partly occupied in a Bidisperse porous medium: Symmetric case. *ASME Jr. of Heat Transfer* 133(2011): 072601.1-072601.9. <https://doi.org/10.1115/1.4003667>

[20] Magyari E. (2013). Normal mode analysis of high speed channel flow in a Bidisperse porous media. *Transport Porous Media* 97(2013): 345-352. <http://dx.doi.org/10.1007/s11242-013-0127-0>

[21] Cheng CY. (2014). Free convection boundary layer flow over a vertical wavy surface embedded in a Bidisperse porous media. *Proceedings for World Congress Engineering* 2(2014): 1381-1386.

[22] Ziyaddin R, Huseyin K. (2007). Two-phase steady flow along a horizontal glass pipe in the presence of the magnetic and electrical fields. *Int. Journal of Heat and Fluid Flow* 29(2007): 263-268. <https://doi.org/10.1016/j.ijheatfluidflow.2007.09.003>

NOMENCLATURE

G	applied pressure gradient	$[Nm^{-2}]$
k_f	permeability of the fracture phase	$[m^2]$
k_p	permeability porous phases	$[m^2]$
r'	dimensional radial coordinate measured from the axis of the tube	$[m]$
R	dimensionless radial coordinate measured from the axis of the tube	$[-]$
a	the radius of the tube	$[m]$
U_f	dimensionless velocity in the fracture phase	$[-]$
U_p	dimensionless velocity in the porous phase	$[-]$
U'_f	dimensional velocity in the fracture phase	$[ms^{-1}]$
U'_p	dimensional velocity in the porous phase	$[ms^{-1}]$
Da_f	Darcy number of the fracture phase	$[-]$
Da_p	Darcy number of the porous phase	$[-]$

Greek symbols

μ	fluid viscosity	$[kgm^{-1}s^{-1}]$
$\bar{\mu}_f$	effective viscosity of the fluid in the fracture	$[kgm^{-1}s^{-1}]$
$\bar{\mu}_p$	effective viscosity of the fluid in the porous phase	$[kgm^{-1}s^{-1}]$
ζ	dimensional coefficient of momentum transfer between fracture and the porous phases	$[kgm^{-3}s^{-1}]$
η	dimensionless coefficient of momentum transfer between fracture and the porous phases	$[-]$
γ_f	ratio of viscosities of the fracture phases	$[-]$
γ_p	ratio of viscosities of the porous phases	$[-]$

Superscript

' dimensionless quantity

Subscripts

f fracture phase
p porous phase

Table 1. Flow pattern in channel and tube with respect to the variation η

η	R	Magyari [20]		Present work	
		p-phase	f-phase	p-phase	f-phase
1.0	0.2	0.0837	0.0107	0.0757	0.0106
	0.4	0.0784	0.0106	0.0702	0.0105
	0.6	0.0670	0.0104	0.0590	0.0102
	0.8	0.0443	0.0090	0.0381	0.0087
2.0	0.2	0.0785	0.0113	0.0718	0.0112
	0.4	0.0738	0.0112	0.0668	0.0110
	0.6	0.0635	0.0108	0.0564	0.0106
	0.8	0.0423	0.0093	0.0367	0.0090
3.0	0.2	0.0741	0.0118	0.0683	0.0116
	0.4	0.0699	0.0117	0.0638	0.0115
	0.6	0.0604	0.0112	0.0542	0.0110
	0.8	0.0406	0.0095	0.0355	0.0092

APPENDIX

$$d_1 = \left(\frac{1}{\eta} \left(\frac{\gamma_f}{\gamma_p D a_p} - \frac{1}{D a_f} \right) + \frac{\gamma_f - \gamma_p}{\gamma_p} \right)$$

$$d_2 = \sqrt{\left(\frac{1}{\eta} \left(\frac{\gamma_f}{\gamma_p D a_p} - \frac{1}{D a_f} \right) + \frac{\gamma_f - \gamma_p}{\gamma_p} \right)^2 + \frac{4\gamma_f}{\gamma_p}}$$

$$d_3 = \frac{\gamma_f + A_1 \gamma_p}{\delta_1^2 \gamma_f \gamma_p}$$

$$d_4 = \frac{\gamma_f + A_2 \gamma_p}{\delta_2^2 \gamma_f \gamma_p}$$

$$d_5 = \frac{1}{\sqrt{\gamma_f D a_f}}$$

$$d_6 = \frac{1}{\sqrt{\gamma_p D a_p}}$$

$$d_7 = \left[\frac{\gamma_f D a_f + \gamma_p D a_p}{\gamma_f \gamma_p D a_f D a_p} \right]$$